Progress In Electromagnetics Research C, Vol. 66, 29–38, 2016

Integrated Filtering Antenna Based on D-CRLH Transmission Lines for Ultra-Compact Wireless Applications

Mahmoud A. Abdalla* **and Ahmed Fouad**

Abstract—This paper presents an ultra-compact filtering integrated antenna for GPS (1.57 GHz) and LTE (2.65 GHz) applications. The antenna comprises integration between dual composite right/left-handed antenna and bandstop filter in one platform. The whole integrated antenna size is only $30 \times 28.5\,\text{mm}^2$. Compared to conventional antenna with the same dimensions, the proposed antenna is only 6.5% at GPS band and 16.5% at LTE band. The deign procedures of individual antennas, bandstop filter and the filtering integrated antennas are explained in details. The full wave simulations supporting the design procedures and experimental measurements for all introduced components are introduced with good agreement. Finally, as a consequence of the proposed antenna ultra small size and its filtering capability, the antenna is a good candidate for implanted antenna applications.

1. INTRODUCTION

The rapid growth of the wireless communication systems leads to integrated different wireless applications in one terminal despite different applications have been assigned different frequencies. One solution is to use multi-band components. Also, the need for these devices to be compact is another challenge, especially for implanted antennas. However, multi-band antennas may suffer from higher order resonance which will reduce the signal to noise figure. One solution is to integrate the antenna with filtering stage [1–4], and another approach is to integrate the filter within the antenna structure [5–7]. The design of filtering antenna has a tradeoff between the design complexity for arbitrary frequencies and the overall antenna size. The integrating approach is a more flexible design and effective at arbitrary frequencies, but the challenge is in the small size of the integrated filter so that the overall noise figure of the whole system will not be affected.

Metamaterials composite right/left-handed transmission lines (CRLH TL) [8], also referred as negative refractive index transmission lines [9], have unique nonlinear frequency dependent sub-wavelength impedance/phase electromagnetic wave propagation. Thanks to these properties many compact and multi-band antennas have been realized, especially at low microwave frequencies, using CRLH TLs. Based on CRLH TL, many ultra-compact multi-band antennas [10–16] and bandstop filters [17, 18] have been reported. Also, some different design integrated filtering antennas have been presented in [19–22]. However, realizing CRLH TL requires shunt connection for inductive load which becomes not simple in practical configurations.

The dual CRLH TL has been suggested as a complement of the CRLH [23]. The D-CRLH TL realization is simpler than CRLH TL since it needs no via connection requirements [24–26]. Similarly, D-CRLH TL opposes nonlinear propagation phase and impedance which make them suitable for compact devices. Furthermore, in an unbalanced D-CRLH TL, there is a sharp cut pass band-stop band transition between the low frequency right-handed and high frequency left-handed compared to the CRLH TL. Many high selective microwave components have been proposed based on D-CRLH cells

Received 8 May 2016, Accepted 1 July 2016, Scheduled 14 July 2016
* Corresponding author: Mahmoud Abdelrahman Abdalla (maaabdalla@ieee.org).
The authors are with the Electromagnetic Fields Group, Electronic Engineering Department, MTC College, Cairo, Egypt.

such as impedance inverters [27] resonator [28, 29] diplexer [30, 31], bandpass filter [32, 33] and bandstop filter [34]. Also, a few attempts have been reported to use D-CRLH cells in antennas [35–37].

In this paper, we introduce an ultra-compact dual-band integrated filtering antenna based on D-CRLH TL configuration. The dual bands are designed to be suitable for GPS (1.57 GHz) and LTE (2.65 GHz). The integrated antenna is printed on a low cost FR4 substrate with 1.6 mm thickness and $\tan\delta = 0.02$ in microstrip configuration. The design principles for the D-CRLH antenna and bandstop filter are introduced. The simulated and measured results for individual and integrated components are disused.

2. ANALYSIS AND DESIGN PROCEDURES

2.1. The D-CRLH Filtering Antenna Principles

A block diagram for the integrated filtering antenna is shown in Fig. 1(a). The filtering antenna was designed using two cascaded sections of different D-CRLH unit cells forming antenna and filter. The equivalent circuit of the D-CRLH TL unit cell is shown in Fig. 1(b). The circuit consists of a transmission line, of electrical length = (θ), loaded with a series tank circuit (the capacitor C_R and the inductor L_L) and a shunt tank circuit (the capacitor C_L and the inductor (L_L)). The propagation along this TL has been explained using the periodic analysis of infinite number of cells of length (d), to be as [9]

$$\cos(\beta d) = \cos(\theta) + \frac{1}{2} ZY \cos^2\left(\frac{\theta}{2}\right) + i\frac{1}{2}\left(Z_o Z + Y_o Y\right)\sin\left(\frac{\theta}{2}\right) \tag{1}$$

where, Z_0 and Y_0 are the RH characteristic impedances and admittances, respectively; Z is the series branch impedance; Y is the shunt branch admittance; θ is the electrical length of the hosting transmission line. Also, the characteristic impedance for the D-CRLH TL can be written as [23]

$$Z_{\text{CRLH}} = \sqrt{\frac{Z}{Y}} = \sqrt{\frac{j\omega L_R\left(1 - \omega^2 L_L C_R\right)}{j\omega C_R\left(1 - \omega^2 L_R C_L\right)}} \tag{2}$$

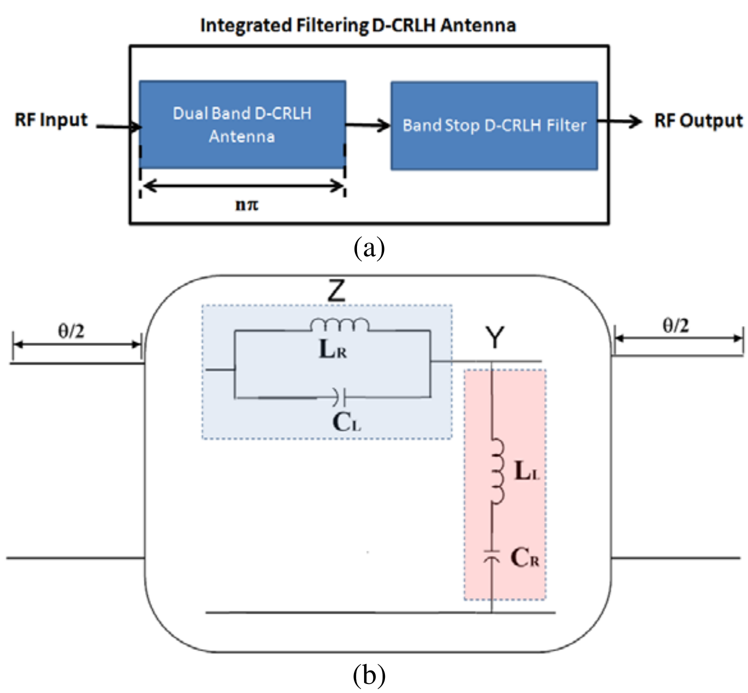

Figure 1. (a) The block diagram of the filtering antenna. (b) The equivalent circuit model of the D-CRLH unit cell.

2.2. The D-CRLH Antenna Design

The detailed geometry for the 2D layout of the dual-band D-CRLH antenna is shown in Fig. 2(a) where it is obvious that the antenna size is only $18 \times 30\,\text{mm}^2$. The fabricated antenna prototype is shown in Fig. 2(b). As shown in the figure, the D-CRLH antenna realization is done by employing one D-CRLH cell fed by a $50\,\Omega$ transmission line. The D-CRLH unit cell is realized using a six-finger interdigital capacitor (C_L) and a high impedance straight line inductance (L_R). The shunt tank circuit connected between the line and ground plane is realized using meander line inductor formed by 6 turns of high impedance lines (L_L) and a wide patch capacitor (C_R).

The idea of using a D-CRLH unit cell for designing a dual-band antenna terminated by an open circuit load can be expressed for a very small periodic cell distance (θ) as

$$\phi_{\text{DCLRH}} = \text{real}\left(\sqrt{ZY}\right) = \text{real}\left(\sqrt{\left(\frac{j\omega L_R}{(1-\omega^2 L_R C_L)}\right)\left(\frac{j\omega C_R}{(1-\omega^2 L_L C_R)}\right)}\right) = n\pi \tag{3}$$

where n is an integer $= 0$ at $f = 1.57\,\text{GHz}$ and $n = 1$ at 2.65 GHz.

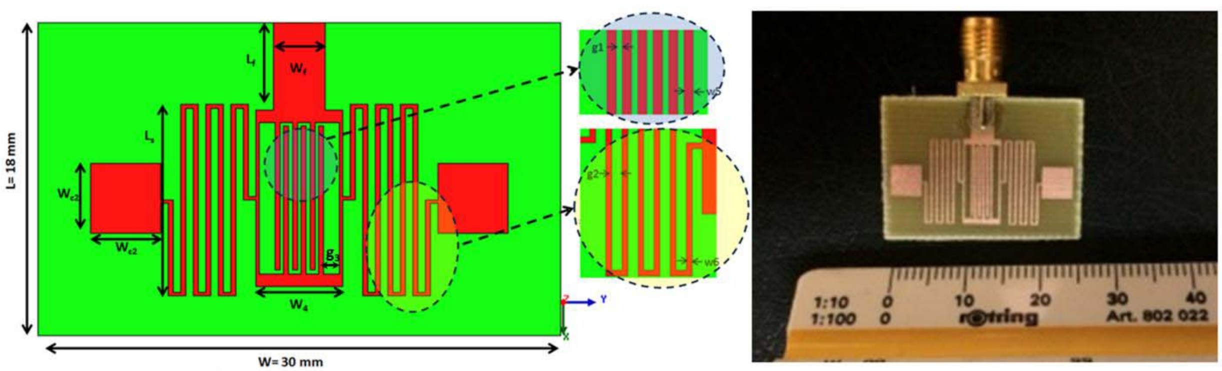

(a) (b)

Figure 2. The dual band DCRLH antenna. (a) The 2D antenna layout, $l_f = 5\,\text{mm}$, $L_{\text{fing}} = 9.5\,\text{mm}$, $g_1 = 0.2\,\text{mm}$, $W_5 = 0.3$, $L_m = 10.9\,\text{mm}$, $W_5 = 0.2\,\text{mm}$, $g_2 = 0.4\,\text{mm}$, $g_2 = 0.85\,\text{mm}$, $W_4 = 5\,\text{mm}$, $W_{c2} = 4.1\,\text{mm}$. (b) The fabricated D-CRLH antenna prototype.

The dimensions of the antenna elements are calculated as

$$C_R = 2\frac{\varepsilon W_{c2}^2}{h} \tag{4a}$$

$$C_L\,(\text{pF}) = 3.937 \times 10^{-5} l_f\,(\varepsilon_r + 1)\,(0.11(n-3) + 0.252) \tag{4b}$$

$$\begin{aligned} L\,(\text{nH}) &= \frac{1}{2} M L_s\,(\text{nH}) \\ L_S\,(\text{nH}) &= 2 \times 10^{-4} L\left(\ln\left(\frac{L}{Wt}\right) + 1.193 + 0.2235\frac{W+t}{L}\right) K_g, \\ K_g &= 0.57 - 0.145\ln\left(\frac{w}{h}\right) \end{aligned} \tag{4c}$$

where l_f is length of line, ε_r the relative permittivity of the substrate, n the number of figures in interdigital capacitor, L_S the inductance of the thin lines, W the width of line, t the metal thickness of line and h the thickness of substrate, and M the number of turns which is 1 for (L_R) and 6 for (L_L). The factor (2) in Equation (4a) and (0.5) in Equation (4c) are due to the parallel connection.

2.3. The D-CRLH Bandstop Filter

The design of the D-CRLH bandstop filter is based on realizing an unbalanced D-CRLH unit cell such that its stopband overlaps with the undesired frequencies in the antenna functionalities. The cut off

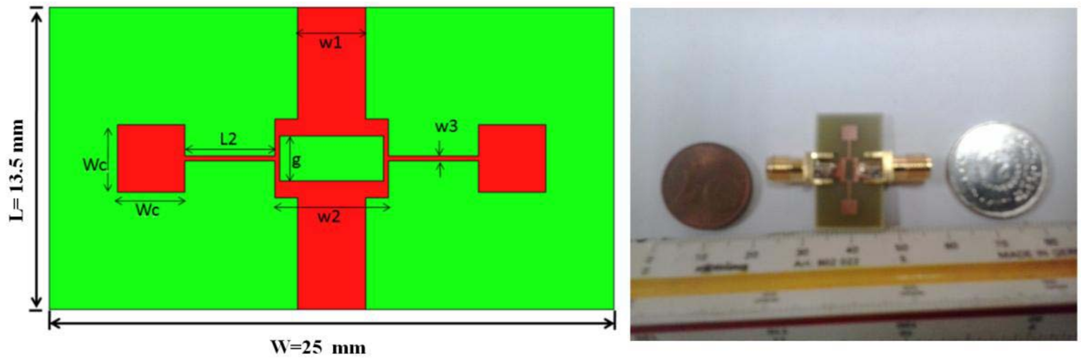

(a)

(b)

Figure 3. The band stop D-CRLH filter. (a) The filter 2D layout, $L = 13.5\,\text{mm}$, $W = 25\,\text{mm}$, $W_1 = 3\,\text{mm}$, $W_2 = 4.5\,\text{mm}$, $W_3 = 0.2\,\text{mm}$, $g_1 = 2\,\text{mm}$, $W_c = 3\,\text{mm}$, $L_2 = 5.3\,\text{mm}$. (b) The fabricated filter prototype.

frequencies are obtained either by satisfying the condition $\beta d = \pi$ (f_{c1} and f_{c2}) or $\beta d = 0$ ($f_{c1} f_{c3}$ and f_{c4}) [23]. Accordingly, the cutoff frequencies of this cell are specified. The specification of the filter is to be centered at 4 GHz and has 3 dB cutoff frequencies at 3 GHz and 5 GHz. The filter layout is shown in Fig. 3(a). In the figure, the filter layout is chosen to realize C_L as an air gap capacitor. The reason behind this element selection is to reduce the effect of parasitic elements and simplify the design process. Also, the filter should have good matching with $50\,\Omega$ feeding.

3. RESULTS AND DISCUSSION

3.1. The Dual-Band D-CRLH Antenna Results

The simulated and measured reflection coefficients of the designed D-CRLH antenna are shown in Fig. 4. It is very obvious that the antenna has satisfied the design conditions at 1.57 GHz and 2.65 GHz with at least −6 dB reflection coefficient with bandwidth = 70 MHz for the first band and 100 MHz for the second band. The antenna has many harmonics at higher frequencies, (at 3.6 GHz, 4.3 GHz and 5.8 GHz, the reflection coefficients are −16 dB, −6 dB and −25 dB, respectively) which may decrease the signal to noise ratio at the two desired frequencies (1.57 GHz and 2.65 GHz). Also, it is clear that a good agreement between the measured and simulated results is achieved.

Comparing the reported antenna size to conventional microstrip antenna size, we can tell that our

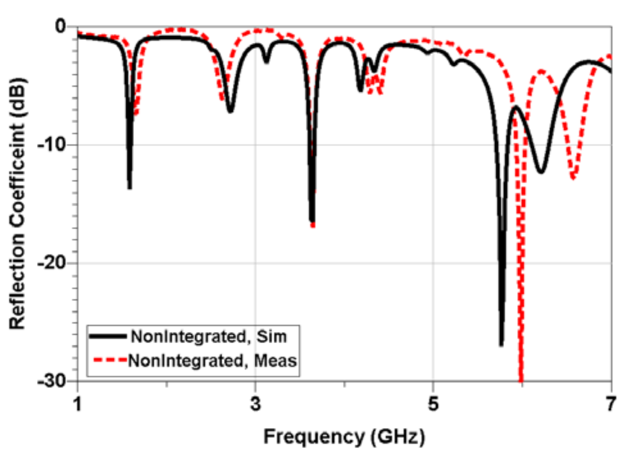

Figure 4. The measured ans simulated reflection coefficient of the DCRLH antenna.

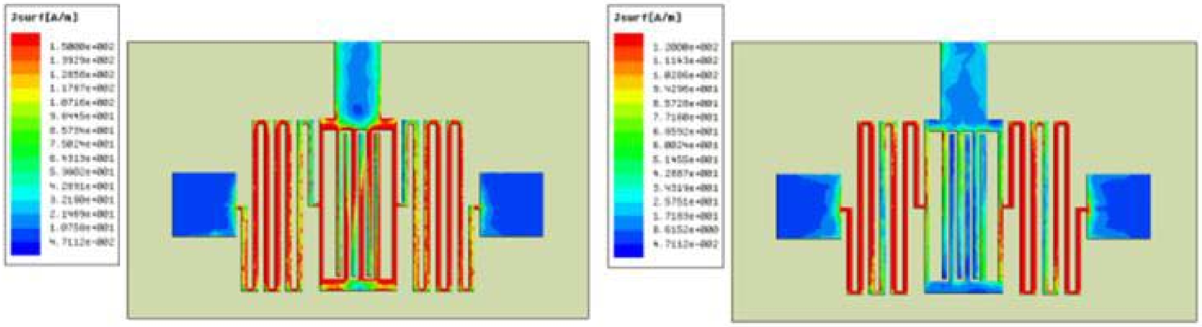

(a) (b)

Figure 5. The simulated current distribution along the dual band D-CRLH antenna, at (a) 1.57 GHz, (b) 2.65 GHz.

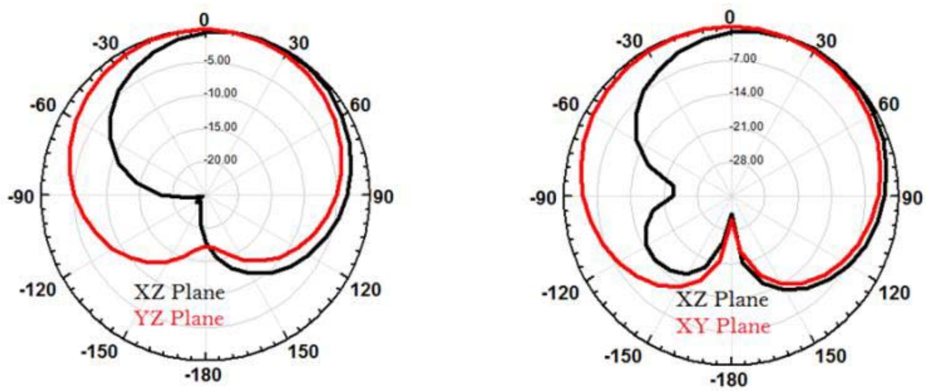

(a) (b)

Figure 6. The $E\,(XZ)$ plane and $H\,(YZ)$ plane 2D normzliaed radiation pattern of the D-CRLH antenna at (a) 1.57 GHz, (b) 2.65 GHz.

antenna size is only 3%, and 9%, compared to conventional microstrip patch antenna with 5 mm feed, at 1.57 GHz (136×100 mm), and 2.65 GHz ($80 \times 65\,\mathrm{m}^2$), respectively [38]. This can confirm the claim that the reported antenna is a good candidate for implanted antenna applications.

The radiation mechanism can be understood by demonstrating the current distribution at the resonant frequencies, for the same current levels and the associated radiation pattern. These simulated results are plotted in Fig. 5. As can be seen, most of the current distribution along the D-CRLH unit cell at 1.57 GHz is concentrated at the interdigital capacitor which means that D-CRLH series capacitor is the parameter that has the greatest effect on this band. In other words, the antenna is resonating as a consequence of the series branch. At 2.65 GHz, most of the current distribution is concentrated at the 6 turns mender lines which make the D-CRLH shunt inductance be the dominant parameter.

The normalized simulated 2D normalized radiation patterns of the triple-band D-CRLH TL antenna in both E plane (XZ plane) and H plane (YZ plane) at 1.57 GHz and 2.65 GHz are shown in Fig. 6(a) and Fig. 6(b), respectively. As shown in the figure, the antenna has a good broadside radiation pattern at different operating bands, which is close to that of the conventional microstrip patch antenna.

3.2. The Dual-Band D-CRLH Band Stop Filter Results

In order to get ride of the higher order harmonics at the antenna response shown in Fig. 4, a bandstop filter was suggested to suppress them. The simulated and measured scattering parameter magnitudes are shown in Fig. 7. As shown in the figure, the filter has bandstop at 4 GHz at which the transmission coefficient (S_{21}) is below -30 dB. The -3 dB transmission coefficient frequencies are at 3 GHz and

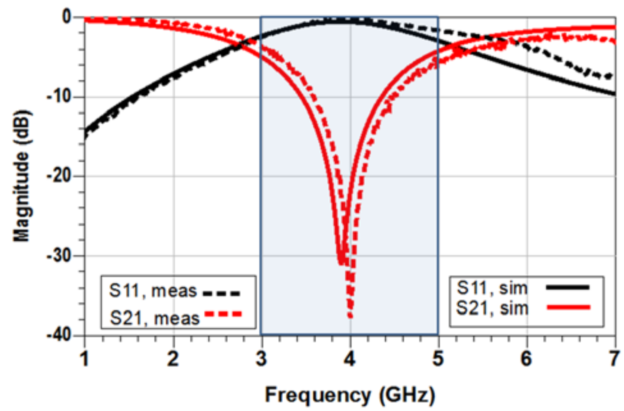

Figure 7. The simulated and measured scattering parameter magnitudes of the D-CRLH bandstop filter.

5 GHz, approximately. It is worth to comment that there is very good agreement between the simulated and measured results. Also, the filter filter length is only $0.0875\,\lambda_g$ where g is guided wavelength at 4 GHz.

4. INTEGRATED D-CRLH ANTENNA STRUCTURE AND RESULTS

Based on the previously reported results for the designed antenna and filter, by integrating them in one platform, a filtering effect can be achieved for the undesired signals at frequencies above 2.65 GHz. Also, thanks to the ultra-small size of the designed filter, the performance of the antenna would be enhanced. The layout of the integrated filtering antenna is shown in Fig. 8(a), and the fabricated prototype is shown in Fig. 8(b). The filtering antenna size is ($30 \times 28.5\,\text{mm}^2$). It is worth to comment that the integrated filtering antenna is still smaller than the conventional non-filtering patch antenna. As pointed out earlier, the size of a conventional single-band microstrip antenna operating at 1.57 GHz or 2.65 GHz, with 5 mm feed, is ($136\times100\,\text{mm}^2$), and ($80\times65\,\text{mm}^2$), respectively. In other words, we can claim that the integrated antenna size is only 6.5% and 16.5%, at 1.57 GHz and 2.65 GHz, respectively, compared to patch antenna at the same frequencies. Therefore, the integrated filtering antenna is still a candidate for implanted antenna applications.

The simulated and measured reflection coefficients of the integrated structure is shown in Fig. 9.

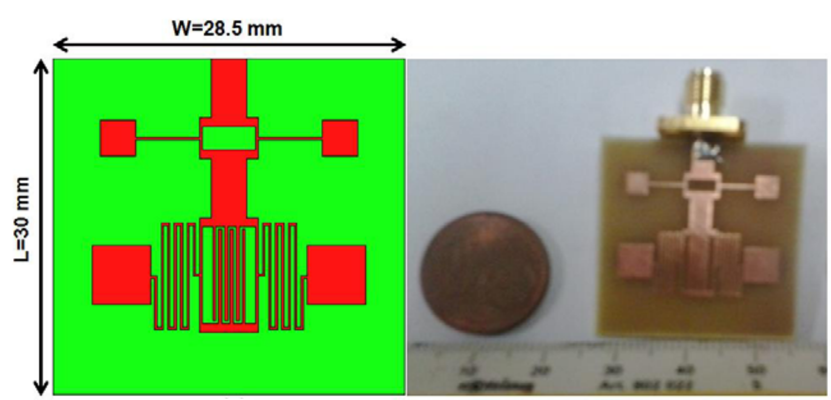

(a) (b)

Figure 8. The integrated D-CRLH filtering antenna. (a) The antenna 2D layout. (b) The fabricated prototype.

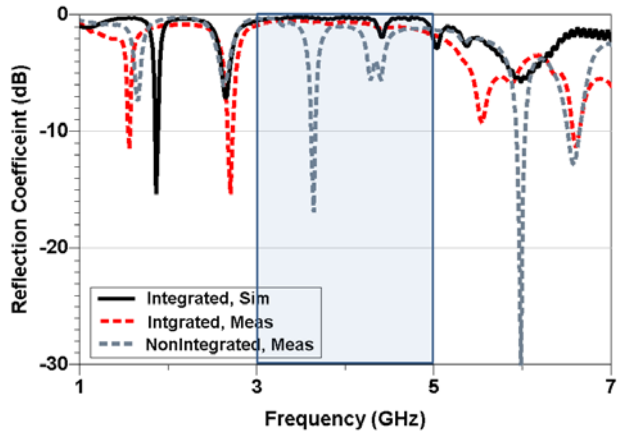

Figure 9. The measured ans simulated reflection coefficeint of the integrated antenna in addition to the measured nonintegrated antenna.

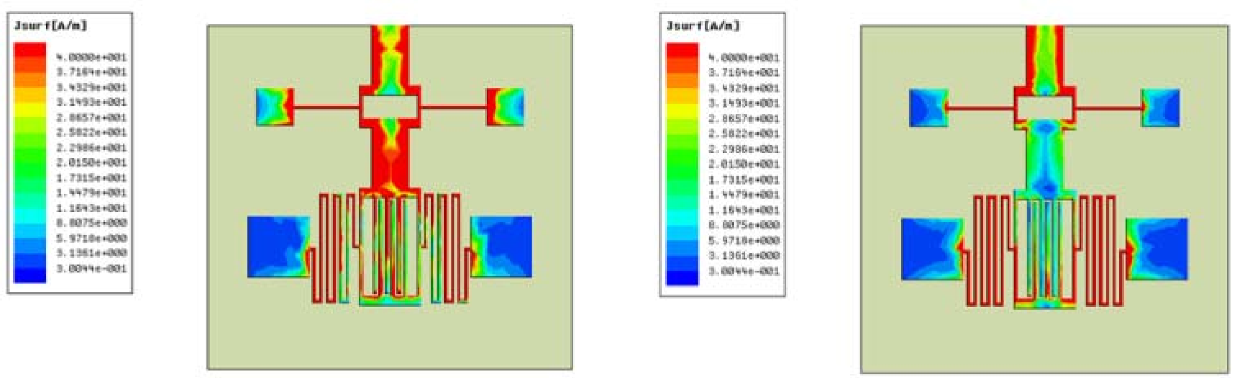

(a) (b)

Figure 10. The current distribution along the integrating filtering dual band antenna (a) at 1.57 GHz and (b) at 2.65 GHz.

In the figure, a reasonable agreement between the two results is achieved. However, there is some frequency shift between the two results at the first band since the the measured reflection coefficient is shifted to 1.8 GHz instead of 1.57 GHz. This can be claimed due to some imperfection in the fabrication process and substrate type which was not possible to be avoided by multiple fabrication. However, at the second band (2.65 GHz), there is very good agreement between the two results.

By emphasizing the frequency band 3 GHz–5 GHz, we can find that there is a successful suppression of unwanted signals if a non-filtering D-CRLH antenna is used. This has been made clearer by adding the measured reflection coefficient of the non-integrated antenna to the same figure. It can be observed that the reflection coefficient of the integrated antenna at 3.6 GHz and 4.3 GHz is only −1 dB instead of −16 dB and −6 dB at the same frequencies of the non-integrated antenna. Beyond 5 GHz, the same responses of the two antennas are the same as consequence of the designed D-CRLH bandstop ending (3 GHz–5 GHz). This can confirm the success of the integrated filter with the single antenna.

To confirm that the integration process has not changed the antenna radiation mechanism, the current distributions along the filtering integrated structure are shown in Fig. 10 at 1.57 GHz and 2.65 GHz. As shown in the figure, the integrated antenna preserves the same resonance along the antenna DCRLH cell similar to the single element previously illustrated in Fig. 5.

Finally, the broadside radiation of the filtering integrated antenna is checked by plotting the normalized radiation pattern at 1.57 GHz and 2.65 GHz in both E and H planes as shown in Fig. 11. We can claim that the filtering antenna preserves a typical broadside pattern the same as the individual antenna previously shown in Fig. 6.

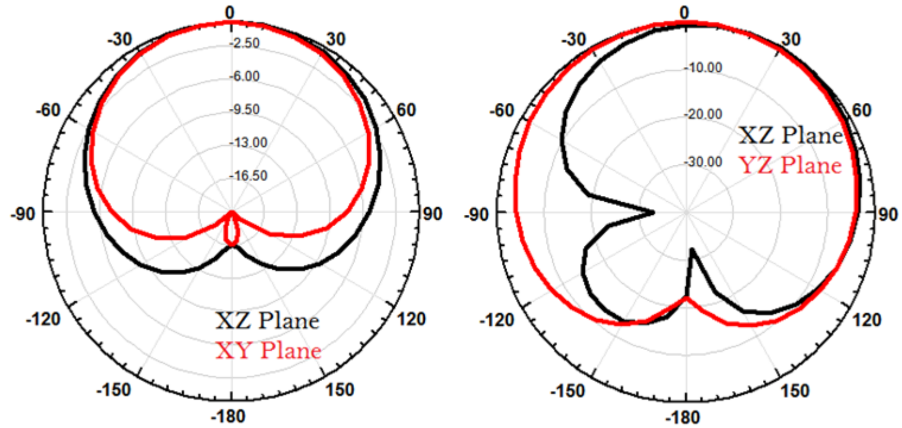

Figure 11. The $E\,(XZ)$ plane and $H\,(YZ)$ plane 2D normzliaed radiation pattern of the integrated DCRLH antenna at (a) 1.57 GHz, (b) 2.65 GHz.

5. CONCLUSION

An integrated compact size dual-band filtering antenna based on D-CRLH metamaterial configuration is introduced. The integrated filtering antenna was designed to have dual bands at 1.57 GHz and 2.65 GHz for the applications of GPS and LTE, respectively with band rejecting any undesired signal up to 6 GHz. The antenna size is only 6.5% and 16.5 % compared to conventional single-band and not filtering microstrip antennas at 1.57 GHz and 2.65 GHz, respectively. The antenna is very powerful in implanted applications. The analysis, full wave simulation and experimental measurements of the individual antenna, filter and also the integrated filtering antenna are introduced. Good matching among all presented results is achieved.

REFERENCES

1. Chuang, C.-T. and S.-J. Chung, "A compact printed filtering antenna using a ground-intruded coupled line resonator," *IEEE Transactions on Antennas and Propagation*, Vol. 59, No. 10, 3630–3637, 2011.
2. Wu, W.-J., Y.-Z. Yin, S.-L. Zuo, Z.-Y. Zhang, and J.-J. Xie, "A new compact filter-antenna for modern wireless communication systems," *IEEE Antennas and Wireless Propagation Letters*, Vol. 10, 1131–1134, 2011.
3. Sun, G.-H., S.-W. Wong, L. Zhu, and Q.-X. Chu, "A compact printed filtering antenna with good suppression of upper harmonic band," *IEEE Antennas and Wireless Propagation Letters*, Vol. 15, 1349–1352, 2016.
4. Hsieh, C.-Y., C.-H. Wu, and T.-G. Ma, "A compact dual-band filtering patch antenna using step impedance resonators," *IEEE Antennas and Wireless Propagation Letters*, Vol. 14, 1056–1059, 2015.
5. Ushijima, Y., T. Sakamoto, E. Nishiyama, M. Aikawa, and I. Toyoda, "5.8-GHz integrated differential rectenna unit using both-sided MIC technology with design flexibility," *IEEE Transactions on Antennas and Propagation*, Vol. 61, No. 6, 3357–3360, 2013.
6. Li, Y., L. Li, Y. Zhang, and C. Zhao, "Design and synthesis of multilayer frequency selective surface based on antenna-filter-antenna using Minkowski fractal structures," *IEEE Transactions on Antennas and Propagation*, Vol. 63, No. 1, 133–141, 2015.
7. Chen, X., F. Zhao, L. Yan, and W. Zhang, "A compact filtering antenna with flat gain response within the passband," *IEEE Antennas and Wireless Propagation Letters*, Vol. 12, 857–860, 2013.

8. Caloz, C. and T. Itoh, *Electromagnetic Metamaterials Transmission Line Theory and Microwave Applications*, John Wiley & Sons, New Jersey, 2006.
9. Eleftheriades, G. V. and K. G. Balmain, *Negative Refractive Metamaterials*, John Wiley & Sons, New Jersey, 2005.
10. Lee, W. H., A. Gummalla, and M. Achour, "Small antennas based on CRLH structures: Concept, design, and applications," *IEEE Ant. and Prop. Mag.*, Vol. 53, No. 2, 10–25, 2011.
11. Ziolkowski, R. W., P. Jin, and C. Lin, "Metamaterial-inspired engineering of antennas," *IEEE Proceedings*, Vol. 99, No. 10, 1720–1731, 2011.
12. Dong, Y. and T. Itoh, "Metamaterial-based antennas," *IEEE Proceedings*, Vol. 100, No. 7, 2271–2285, 2012.
13. Abdalla, M. A., A. A. Ibrahim, and M. H. Abd El-Azeem, "Phase enhancement for multi-resonance compact metamaterial antennas," *Progress In Electromagnetic Research C*, Vol. 60, 83–93, 2015.
14. Abdalla, M. A. and M. A. Fouad, "CPW dual-band antenna based on asymmetric generalized metamaterial π NRI transmission line for ultra compact applications," *Progress In Electromagnetic Research C*, Vol. 62, 99–107, 2016.
15. Abdalla, M. and F. H. Sadek, "Compact triple-band left-handed antenna for GSM/WiMAX applications," *2015 9th International Congress on Advanced Electromagnetic Material in Microwave and Optics*, 295–297, UK, 2015.
16. Abdalla, M. and A. Ibrahim, "Multi-band meta-material antenna with asymmetric coplanar strip-fed structure," *2015 IEEE AP-S Int. Antenna and Propagation Symposium Digest*, 631–632, Canada, 2015.
17. Song, K., T. Pan, Y. Fan, and C. Zhong, "Wideband CRLH-transmission line bandstop filter," *2012 10th International Symposium on IEEE Antennas, Propagation & EM Theory (ISAPE)*, 1192–1194, 2012.
18. Abdalla, M. A., M. A. Fouad, H. A. Elregeily, and A. A. Mitkees, "Wideband negative permittivity metamaterial for size reduction of stopband filter in antenna applications," *Progress In Electromagnetics Research C*, Vol. 25, 55–66, 2012.
19. Abdalla, M., S. Karimian, and Z. Hu, "Dual band spurious-free SIR metamaterial antenna," *2014 IEEE AP-S International Antenna and Propagation Symposium Digest*, 1005–1006, Memphis, USA, 2014.
20. Abdalla, M. A., A. A. Awad, and K. M. Hassan, "Wide band high selective compact metamaterial antenna for 2 GHz wireless applications," *2014 Loughborough Antennas & Propagation Conference*, 350–354, Loughborough, UK, 2014.
21. Abdalla, M., M. A. El-Dahab, and M. Ghouz, "SIR double periodic CRLH loaded dipole antenna," *2015 IEEE AP-S International Antenna and Propagation Symposium Digest*, 832–833, Canada, July 2015.
22. Chen, L.-N. and Y.-L. Luo, "Compact filtering antenna using CRLH resonator and defected ground structure," *Electronics Letters*, Vol. 50, No. 21, 1496–1498, 2014.
23. Caloz, C., "Dual composite right/left-handed (D-CRLH) transmission line metamaterial," *IEEE Microwave and Wireless Components Letters*, Vol. 16, No. 11, 585–587, 2006.
24. Belenguer, A., J. Cascon, A. L. Borja, H. Esteban, and V. E. Boria, "Dual composite right-/left-handed coplanar waveguide transmission line using inductively connected split-ring resonators," *IEEE Transactions on Microwave Theory and Techniques*, Vol. 60, No. 10, 3035–3042, 2012.
25. Belenguer, A., A. L. Borja, and V. E. Boria, "Balanced dual composite right/left-handed microstrip line with modified complementary split-ring resonators," *IEEE Antennas and Wireless Propagation Letters*, Vol. 12, 880–883, 2013.
26. Colin, D. D. and Z. Hu, "Uniplanar metamaterial based dual composite right-/left-handed (D-CRLH) microstrip line for microwave circuit applications," *2014 Asia-Pacific Microwave Conference (APMC)*, 211–213, 2014.
27. Ikholodnyak, D., V. Turgaliev, and E. Zameshaeva, "Dual-band immittance inverters on dual-composite right/left-handed transmission line (D-CRLH TL)," *2015 German Microwave*

Conference (GeMiC), 60–63, 2015.

28. Daw, A. F., M. A. Abdalla, and H. M. Elhennawy, "Dual band high selective compact transmission line gap resonator," *2014 Loughborough Ante. & Propagation Conference*, 91–94, UK, 2014.
29. Daw, A. F., M. A. El Rahman Abdalla, and H. M. El Hennawy, "Multiband sharp-skirt compact gap resonator based D-CRLH," *2015 32th National Radio Science Conference (NRSC 2015)*, 43–50, Egypt, 2015.
30. González-Posadas, V., J. L. Jiménez-Martín, A. Parra-Cerrada, L. E. Garcıa-Munıoz, and D. Segovia-Vargas, "Dual-composite right-left-handed transmission lines for the design of compact diplexers," *IET Microwaves, Antennas & Propagation*, Vol. 4, No. 8, 982–990, 2010.
31. Mocanu, I. A. and G. Sajin, "The study of different types of D-CRLH transmission lines for microwave diplexer," *2013 IEEE EUROCON*, 1849–1852, 2013.
32. Tong, W., Z. Hu, H. Zhang, C. Caloz, and A. Rennings, "Study and realisation of dual-composite right/left-handed coplanar waveguide metamaterial in MMIC technology," *IET Microwaves, Antennas & Propagation*, Vol. 2, No. 7, 731–736, 2008.
33. Jang, G. and S. Kahng, "Design of a dual-band metamaterial bandpass filter using zeroth order resonance," *Pogress In Electromagnetics Research C*, Vol. 12, 149–162, 2010.
34. Wu, G.-C., G.-M. Wang, T. Li, and C. Zhou, "Novel dual-composite right/left-handed transmission line and its application to bandstop filter," *Progress In Electromagnetics Research Letters*, Vol. 37, 29–35, 2013.
35. Liu, C.-Y., Q.-X. Chu, and J.-Q. Huang, "A planar D-CRLH transmission line structure and its application to leaky-wave antenna," *9th Int. Symp. on Ant., Prop. and EM The. (ISAPE)*, 345–348, 2010.
36. Quang, H. N. and H. Shirai, "A compact tri-band metamaterial antenna for WLAN and WiMAX applications," *2015 International Conference on Electromagnetics in Advanced Applications (ICEAA)*, 133–136, 2015.
37. Abdalla, M. and A. Fouad, "Compact triple band D-CRLH metamaterial antenna," *2015 IEEE AP-S Int. Antennas and Propagation Symposium Digest*, 1190–1191, Canada, 2015.
38. Balanis, C. A., *Antenna Theory: Analysis and Design*, 4th edition, Wiley and Sons, 2016.